Exact ground-state properties of the SU(2) Hamiltonian lattice gauge theory

S. A. Chin*
Department of Physics, University of California at Los Angeles, Los Angeles, California 90024

O. S. van Roosmalen,† E. A. Umland, and S. E. Koonin
W. K. Kellogg Radiation Laboratory, California Institute of Technology, Pasadena, California 91125
(Received 7 January 1985)

The SU(2) Hamiltonian lattice gauge theory is shown explicitly to be equivalent to a nonrelativistic quantum many-body problem in S^3. By exploiting this equivalence, a many-body Monte Carlo algorithm is devised to solve for its ground-state properties. To the extent that a trial wave function consisting of a product of single-plaquette functions is a good approximation to the exact ground state, the present Monte Carlo method is shown to be an efficient means of calculating the ground-state energy with high precision.

I. INTRODUCTION

The Monte Carlo method[1] is currently an indispensable numerical tool for investigating the nonperturbative properties of lattice gauge theories. Physical observables[1] such as the string tension, the heavy-quark potential, the glueball mass, and the deconfinement temperature are of direct relevance for the studies of quark confinement, hadronic spectroscopy, and ultrarelativistic heavy-ion collisions. The Lagrangian formulation of lattice gauge theories reduces the study of quantum field theories to that of the statistical mechanics of Ising-type models on a four-dimensional space-time lattice. In this approach, the traditional tools of statistical mechanics, including order parameters, renormalization-group transformations, duality arguments, and high-temperature series expansions provide powerful means of elucidating the global critical behavior of these theories. Alternatively, lattice gauge theories can be treated in the Hamiltonian formalism,[2,3] in which the quantum field theory is related to a quantum many-body problem on a three-dimensional spatial lattice. In this case, one is confronted with a familiar Schrödinger eigenvalue problem.

From the perspective of Monte Carlo calculations, there are several advantages to the Hamiltonian formalism. In this formulation, time remains continuous and time intervals are merely parameters which can be extended indefinitely, rather than acting as *a priori* constraints on the temporal size of the lattice. Thus, for reasonably large lattices, the number of degrees of freedom required for a Hamiltonian calculation is significantly less than that for a Lagrangian computation. Furthermore, many physical observables are eigenvalues of a Hamiltonian. They therefore can be evaluated directly and their stationary properties as an eigenvalue can be exploited to reduce statistical fluctuations. In contrast, the Lagrangian formalism requires that physical observables such as the string tension or heavy-quark potential be deduced indirectly from various Wilson loops, with relatively large variances. More importantly, Monte Carlo methods[5–12] for sampling the ground state of a many-body Hamiltonian allow approximate knowledge of the solution to be incorporated via a trial function and only require the stochastic process to deal with that portion of the problem which is not solvable analytically. To the extent that the trial function is a reasonable approximation to the ground state, these methods can be efficient means of calculating exact ground-state properties. Thus, although Lagrangian Monte Carlo computations are extensively performed at present, the inherent numerical efficiency of the Hamiltonian approach deserves to be more widely appreciated.

The utility of using stochastic techniques developed for quantum many-body systems to the study of Hamiltonian lattice gauge theories was first demonstrated in Refs. 4 and 13 for the case of U(1). In Ref. 13, the Green's-function Monte Carlo method[5] was used, while Ref. 4 used guided random walks. In this work, we apply the guided-random-walk algorithm of Ref. 4 to solve for the ground state of the SU(2) lattice gauge theory.

The paper is organized as follows: In Sec. II, we show that if the basic commutators of the theory are realized via differential operators, then the SU(2) lattice gauge theory is equivalent to a nonrelativistic quantum many-body problem in S^3. The specific Monte Carlo algorithm for sampling the ground state is described in Sec. III. Section IV discusses the form of the trial wave function. The variational calculation which fixes the parametrization of the trial function, the exact numerical results for the ground-state energy, and the plaquette expectation value are presented in Sec. V. To check finite-size effects, variational calculations were also performed with the discrete icosahedral subgroup of SU(2) for lattice sizes up to $16\times16\times16$. Conclusions and future applications for evaluating other physical observables are discussed in Sec. VI, while some technical details pertaining to the single-plaquette Hamiltonian, cluster expansion, and the computation of the kinetic (i.e., "electric") energy are contained in the Appendix.

II. SU(2) LATTICE GAUGE THEORY

In a three-dimensional simple cubic lattice with lattice spacing a, the link connecting site $(n_1,a,n_2a,n_3a)\equiv\mathbf{n}a$ with site $\mathbf{n}a+\mathbf{e}_ja$ can be uniquely identified by the lattice

 ©1985 The American Physical Society

vector $\mathbf{n}$ and the direction j. Denoting this combination by a single link index $l=(\mathbf{n},j)$, a triplet of dynamical variables A^a, defined on each link of the lattice, can be labeled $A_j^a(\mathbf{n})$, or more simply, A_l^a. In the SU(2) lattice gauge theory, each *directed* link is associated with an element of SU(2) specified by A_l^a:

$$U_{\pm l}=\exp(\mp i\tfrac{1}{2}\tau^a A_l^a)\ , \tag{2.1}$$

where the plus or minus sign in U further specifies the direction of the given link. For example, U_{-l} is associated with the link $(\mathbf{n},j)$ pointing in the negative-j direction. The τ^a are the usual Pauli matrices and a summation convention has been adopted.

The SU(2) lattice Hamiltonian[2,3] is given by

$$H=\frac{g^2}{a}\left[\sum_l \tfrac{1}{2}E_l^a E_l^a+\lambda\sum_p[1-\cos(\tfrac{1}{2}B_p)]\right]\ , \tag{2.2}$$

where g is the coupling constant,

$$\cos(\tfrac{1}{2}B_p)=\tfrac{1}{2}\mathrm{tr}U_p\ ,$$

$\lambda=4/g^4$, and U_p denotes the product of four U's corresponding to a directed chain of four links around an elementary square or plaquette. The theory is quantized by postulating, for each link, either

$$[E^a,U]=\tfrac{1}{2}\tau^a U \tag{2.3}$$

or

$$[E^a,U]=U\tfrac{1}{2}\tau^a\ , \tag{2.4}$$

thus identifying E^a as either the left or right generator[14] of SU(2).

From the point of view of the U's the A's at each link are merely coordinates that parametrize the group manifold of SU(2). Since

$$U=\exp(-i\tfrac{1}{2}\tau^a A_l^a)=\cos(\tfrac{1}{2}\rho)-i\hat{n}^a\tau^a\sin(\tfrac{1}{2}\rho)\ , \tag{2.5}$$

with $A^a=\rho\hat{n}^a$, $\hat{n}^a=(\sin\theta\cos\phi,\ \sin\theta\sin\phi,\cos\theta)$, $0\le\rho\le 2\pi$, $0\le\theta\le\pi$, and $0\le\phi\le 2\pi$, the set of polar coordinates (ρ,θ,ϕ) is another useful parametrization. In particular, we may label the elements of SU(2) interchangeably as either U or (ρ,θ,ϕ). In terms of (ρ,θ,ϕ), the commutation relations (2.3) and (2.4) can be realized via differential operators acting on the group manifold by requiring, respectively.

$$E_L^a U=\left[f_L^a\frac{\partial}{\partial\rho}+g_L^a\frac{\partial}{\partial\theta}+h_L^a\frac{\partial}{\partial\phi}\right]U=\tfrac{1}{2}\tau^a U \tag{2.6}$$

and

$$E_R^a U=\left[f_R^a\frac{\partial}{\partial\rho}+g_R^a\frac{\partial}{\partial\theta}+h_R^a\frac{\partial}{\partial\phi}\right]U=U\tfrac{1}{2}\tau^a\ . \tag{2.7}$$

By comparing the coefficients of the τ's on both sides of (2.6) and (2.7) the f's, g's, and h's can be determined to give

$$E^1=\tfrac{1}{2}i\left[2\sin\theta\cos\phi\frac{\partial}{\partial\rho}+(\cot\tfrac{1}{2}\rho\cos\theta\cos\phi\pm\sin\phi)\frac{\partial}{\partial\theta}+\left[\pm\cot\theta\cos\phi-\cot\tfrac{1}{2}\rho\frac{\sin\phi}{\sin\theta}\right]\frac{\partial}{\partial\phi}\right]\ , \tag{2.8}$$

$$E^2=\tfrac{1}{2}i\left[2\sin\theta\sin\phi\frac{\partial}{\partial\rho}+(\cot\tfrac{1}{2}\rho\cos\theta\sin\phi\mp\cos\phi)\frac{\partial}{\partial\theta}+\left[\pm\cot\theta\sin\phi+\cot\tfrac{1}{2}\rho\frac{\cos\phi}{\sin\theta}\right]\frac{\partial}{\partial\phi}\right]\ , \tag{2.9}$$

$$E^3=\tfrac{1}{2}i\left[2\cos\theta\frac{\partial}{\partial\rho}-\cot\tfrac{1}{2}\rho\sin\theta\frac{\partial}{\partial\theta}\mp\frac{\partial}{\partial\phi}\right]\ , \tag{2.10}$$

where the upper (lower) sign is for E_R^a (E_L^a). One can check directly that they satisfy the defining Lie algebras of SU(2):

$$[E_L^a,E_L^b]=-i\epsilon_{abc}E_L^c\ , \tag{2.11}$$

$$[E_R^a,E_R^b]=+i\epsilon_{abc}E_R^c\ . \tag{2.12}$$

They are not independent of each other but are related by

$$\tau^a E_L^a=(U\tau^b U^{-1})E_R^b\ . \tag{2.13}$$

If a rotation matrix $R^{ab}(U)$ is defined via

$$\tau^a R^{ab}(U)=U\tau^b U^{-1}\ , \tag{2.14}$$

then (2.13) reads

$$E_L^a=R^{ab}(U)E_R^b\ . \tag{2.15}$$

In the case where the SU(2) group manifold is parametrized by Euler angles, the corresponding expressions for $E_{L,R}^a$ can be found in Ref. 14.

The Casimir operator E^aE^a, which appears in the Hamiltonian, is by virtue of (2.15) the same for either E_L^a or E_R^a:

$$E^aE^a=E_L^aE_L^a=E_R^aE_R^a=-\frac{1}{4\sin^2(\frac{1}{2}\rho)}\left[\frac{\partial}{\partial\rho}\left[4\sin^2(\tfrac{1}{2}\rho)\frac{\partial}{\partial\rho}\right]+\frac{1}{\sin\theta}\frac{\partial}{\partial\theta}\left[\sin\theta\frac{\partial}{\partial\theta}\right]+\frac{1}{\sin^2\theta}\frac{\partial^2}{\partial\phi^2}\right]\ , \tag{2.16}$$

which is simply the Laplace-Beltrami operator $-\Delta$ on S^3 with metric

$$ds^2=d\rho^2+4\sin^2(\tfrac{1}{2}\rho)(d\theta^2+\sin^2\theta\, d\phi^2). \tag{2.17}$$

By scaling out the lattice spacing a via $H\rightarrow g^2H/a$, one obtains a dimensionless Hamiltonian in the form

$$H=-\tfrac{1}{2}\sum_l \Delta_l+\lambda\sum_p[1-\cos(\tfrac{1}{2}B_p)]\ . \tag{2.18}$$

In this case, one can regard (2.18) as describing a quantum system of nonrelativistic particles in S^3, each labeled by $l=(\mathbf{n},j)$ with "coordinate" (ρ_l,θ_l,ϕ_l), interacting with each other through a sum of four-body potentials $V\{\rho_l,\theta_l,\phi_l\}=\lambda\sum_p[1-\cos(\frac{1}{2}B_p)]$. From this perspective, the dynamics takes place entirely in the group manifold and the underlying lattice structure serves merely to identify the participants of each four-body interaction. In the extreme limit of $\lambda=0$, the eigenfunctions of H are simply products of individual link states, $\prod_l|U_l\rangle$, where $\langle jmm'|U_l\rangle=D^j_{mm'}(\rho_l,\theta_l,\phi_l)$ are the well-known complete set of states[14] of SU(2), labeled by the eigenvalues of $-\Delta\ [=j(j+1)]$, $E^3_L\ (=m)$, and $E^3_R\ (=m')$.

The Hamiltonian (2.18) commutes with time-independent gauge transformations parametrized by an arbitrary function $\omega^a(\mathbf{n})$:

$$\Omega[\omega^a(\mathbf{n})]=\exp\left[i\sum_n\omega^a(\mathbf{n})\sum_{j=1}^3[E^a_{Lj}(\mathbf{n})-E^a_{Rj}(\mathbf{n}-\mathbf{e}_j)]\right]. \tag{2.19}$$

The effect of this is to multiply each U on the positive direction links of $\mathbf{n}$ *on the left* by $S(\mathbf{n})=\exp[+i\frac{1}{2}\tau^a\omega^a(\mathbf{n})]$ and each U on the negative direction links of $\mathbf{n}$ *on the right* by $S^{-1}(\mathbf{n})$. The net results is to shift $U_3(\mathbf{n})\rightarrow U'_j(\mathbf{n})=S(\mathbf{n})U_j(\mathbf{n})S^{-1}(\mathbf{n}+e_j)$, which is the correct gauge transformation. Hence eigenstates of H are degenerate with respect to these transformations. For a given eigenvalue of H, one can always choose a gauge invariant eigenstate Ψ such that $\Omega\Psi\{U_l\}=\Psi\{U_l\}$. In this case, Ψ is annihilated by all of the generators of (2.19),

$$\sum_{j=1}^3[E^a_{Lj}(\mathbf{n})-E^a_{Rj}(\mathbf{n}-\mathbf{e}_j)]\Psi=0\ . \tag{2.20}$$

For weak coupling, corresponding to the continuum limit,

$$R^{ab}(U)=\tfrac{1}{2}\mathrm{tr}(\tau^aU\tau^bU^{-1})$$
$$=\delta^{ab}+g\epsilon^{cba}A^c+\cdots\ , \tag{2.21}$$

and (2.20) reduces to

$$(\nabla_jE^a_j+g\epsilon^{abc}A^b_jE^c_j)\Psi=0\ , \tag{2.22}$$

where E^a can either be E^a_L or E^a_R. Consequently, only gauge invariant eigenstates of H, which obey the above generalization of Gauss's law for a Yang-Mills theory, are physical. Equations (2.18) and (2.20) imply that the SU(2) lattice gauge theory is equivalent to a quantum many-body problem in S^3 with the novel symmetry requirement of gauge invariance.

III. GUIDED RANDOM WALKS

Monte Carlo methods for calculating ground-state properties of many-body systems are essentially stochastic means by which physical observables are evaluated as multidimensional integrals. The method of guided random walks is a specific stochastic algorithm for sampling the ground state wave function via a discretized path integral. In this section, we show how the algorithm is actually implemented to study the SU(2) lattice gauge theory; more detailed discussions of the method can be found in Refs. 4–12.

The ground state $|\Psi_0\rangle$ can be evolved from any initial trial state $|\Phi\rangle$ not orthogonal to $|\Psi_0\rangle$ by the evolution operator $e^{-t(H-E)}$:

$$|\Psi_0\rangle=\lim_{t\rightarrow\infty}e^{-t(H-E)}|\Phi\rangle=\lim_{\substack{\Delta t\rightarrow0\\N\Delta t\rightarrow\infty}}e^{-N\Delta t(H-E)}|\Phi\rangle\ . \tag{3.1}$$

To derive the algorithm, one evolves directly the product $\Phi|\Psi_0\rangle$ by inserting in (3.1) complete sets of states in the form $1=\int d\mathbf{x}\,\Phi^{-1}(\mathbf{x})|\mathbf{x}\rangle\langle\mathbf{x}|\Phi(\mathbf{x})$,

$$\begin{aligned}\Phi(\mathbf{x})\Psi_0(\mathbf{x})&=\langle\mathbf{x}|\Phi|\Psi_0\rangle\\&=\int d\mathbf{x}_N\cdots d\mathbf{x}_0\langle\mathbf{x}|\Phi e^{-\Delta t(H-E)}\Phi^{-1}|\mathbf{x}_N\rangle\\&\quad\times\langle\mathbf{x}_N|\Phi e^{-\Delta t(H-E)}\Phi^{-1}|\mathbf{x}_{N-1}\rangle\cdots\langle\mathbf{x}_1|\Phi e^{-\Delta t(H-e)}\Phi^{-1}|\mathbf{x}_0\rangle\langle\mathbf{x}_0|\Phi|\Phi\rangle\ ,\end{aligned} \tag{3.2}$$

where $\mathbf{x}=\{U_l\}$ denotes an entire lattice configuration, $|\mathbf{x}\rangle=\prod_l|U_l\rangle$, $d\mathbf{x}=\prod_l dU_l$, and $dU=(16\pi^2)^{-1}\times4\sin^2(\frac{1}{2}\rho)d\rho\sin\theta\,d\theta\,d\phi$. For an infinitesimal time step Δt,

$$\langle\mathbf{x}'|\Phi e^{-\Delta t(H-e)}\Phi^{-1}|\mathbf{x}\rangle=\prod_l\langle U'_l|\Phi\exp(-\tfrac{1}{2}\Delta tE^a_lE^a_l)\Phi^{-1}|U_l\rangle e^{\Delta t[E-V(\mathbf{x})]}+O(\Delta t^2)\ . \tag{3.3}$$

The matrix element $\langle U'|\Phi\exp(-\frac{1}{2}\Delta tE^aE^a)\Phi^{-1}|U\rangle$ can be evaluated by expanding the exponential in powers of Δt, commuting all angular momentum operators E^a to the left of all coordinate operators in each term, and reexponentiating. For a detailed discussion of the procedure, see Ref. 15. Denoting this operator ordering by $N\{\ \}$, one finds

$$\Phi\exp(-\tfrac{1}{2}\Delta tE^aE^a)\Phi^{-1}=N\{\exp\{-\tfrac{1}{2}\Delta t[E^aE^a-2E^a(E^a\Phi)\phi^{-1}+(E^aE^a\Phi)\phi^{-1}]+\tfrac{1}{2}\Delta t^2E^aE^b(E^bE^a\ln\Phi)\}+O(\Delta t^2)\}\ , \tag{3.4}$$

where parentheses enclosing E^a mean explicit derivatives on Φ. In practice, the quadratic form $E^aE^b(E^bE^a\ln\Phi)$ can usually be replaced by the dominant diagonal approximation[5-10] $E^aE^b(E^bE^a\ln\Phi)\simeq E^aE^a(\frac{1}{3}E^bE^b\ln\Phi)$, thus yielding

$$\langle x'|\Phi e^{-\Delta t(H-E)}\Phi^{-1}|x\rangle=\prod_l\langle U_l'|N\{\exp(-\tfrac{1}{2}\Delta\tilde{t}E_l^aE_l^a)\exp[\Delta tE_l^a(E_l^a\ln\Phi)]\}|U_l\rangle$$
$$\times\exp\{\Delta t[E-\Phi^{-1}H\Phi(x)]\}+O(\Delta t^2) \tag{3.5}$$
$$=p(x',x)w(x)+O(\Delta t^2) \tag{3.6}$$

with $\Delta\tilde{t}=\Delta t(1-\frac{1}{3}\Delta tE^aE^a\ln\Phi)$.

The guided-random-walks algorithm evaluates the discretized path integral (3.2) stochastically as follows: An ensemble of lattice configurations $\{\mathbf{x}_0\}$ is initially generated according to the distribution $\Phi^2(\mathbf{x}_0)=\langle\mathbf{x}_0|\Phi|\Phi\rangle$ using, for example, the Metropolis[16] method. At the kth time step, the next ensemble $\{\mathbf{x}_{k+1}^i\}$ is evolved from $\{\mathbf{x}_k^i\}$ according to the matrix element $p(\mathbf{x}_{k+1},\mathbf{x}_k)w(\mathbf{x}_k)$. This is accomplished by replicating each $\mathbf{x}_k^i$ configuration $w(\mathbf{x}_k^i)=\exp\{\Delta t[E-\Phi^{-1}H\Phi(\mathbf{x}_k^i)]\}$ times, treating the fractional part of $w(\mathbf{x}_k^i)$ as a probability, and generating a configuration $\mathbf{x}_{k+1}^i$ from each resulting $\mathbf{x}_k^i$ with transition probability $p(\mathbf{x}_{k+1},\mathbf{x}_k)$. The replication process effectively duplicates each configuration $\mathbf{x}_k^i$ stochastically $N_i=\text{integer}[w(\mathbf{x}_k^i)+\xi]$ times, where ξ is a uniform random number in [0,1). If $N_i=0$, then the corresponding configuration is deleted from the ensemble. Since E^a's are the generators of rotation and E^aE^a is the Casimir operator,[17,18]

$$\langle U'|N\{\exp(-\tfrac{1}{2}\Delta\tilde{t}E^aE^a)\exp[-iE^a(i\Delta tE^a\ln\Phi)]\}|U\rangle$$
$$=\langle U'|\exp(-\tfrac{1}{2}\Delta\tilde{t}E^aE^a)|U_dU\rangle=\langle U'(U_dU)^{-1}|\exp(-\tfrac{1}{2}\Delta\tilde{t}E^aE^a)|I\rangle$$
$$=(2\pi\Delta\tilde{t})^{-3/2}e^{\Delta\tilde{t}/8}\sum_{n=-\infty}^{\infty}\frac{\Delta s/2+2\pi n}{\sin(\Delta s/2)}\exp[-2(\Delta s/2+2\pi n)^2/\Delta\tilde{t}]\ , \tag{3.7}$$

$$\lim_{\Delta t\to 0}\to(2\pi\Delta\tilde{t})^{-3/2}\exp(-\Delta s^2/2\Delta\tilde{t})\ ,$$

where $U_d=\exp[i\frac{1}{2}\tau^a(i\Delta tE^a\ln\Phi)]$ and Δs is the distance between U' and U_dU. Hence, each link variable U' in $\mathbf{x}_{k+1}^i$ can be updated from the corresponding U in $\mathbf{x}_k^i$, with the required transition probability (3.7) by setting

$$U'=\Delta UU_dU\ , \tag{3.8}$$

where ΔU is a SU(2) group element Gaussian distributed in distance from the identity with zero mean and variance $\langle\Delta s^2\rangle=\Delta\tilde{t}$. The effect of multiplying U by ΔU and U_d is to translate the position (ρ,θ,ϕ) by a Gaussian random walk plus a drift step guided by the trial function. In the limit of large number of time steps and small step size, this procedure will evolve, according to (3.2), to an ensemble of lattice configurations with distribution $\Phi(\mathbf{x})\Psi_0(\mathbf{x})$.

Once the ensemble has evolved long enough to reach the stationary distribution $\Phi(\mathbf{x})\Psi_0(\mathbf{x})$, the ground-state energy E_0 can be determined as that value of E in (3.2) which keeps the ensemble population stable in successive time steps. Alternatively, E_0 can be calculated directly from the ensemble configurations via

$$E_0=\frac{\langle H\Phi|\Psi_0\rangle}{\langle\Phi|\Psi_0\rangle}=\lim_{n\to\infty}\frac{1}{n}\sum_{i=1}^{n}\Phi^{-1}H\Phi(\mathbf{x}^i)\ . \tag{3.9}$$

The value of E_0 determined by these two methods is referred to as the normalization (E_N) and trial (E_T) energy, respectively. Their agreement in the limit of $\Delta t\to 0$ is a necessary consistency test of the entire Monte Carlo algorithm.

The evaluation of the ground-state energy via (3.9) fully exploits the fact that E_0 is an eigenvalue of H. If Φ were the exact ground state, (3.9) would yield E_0 exactly with zero variance, independent of the statistical fluctuations or systematic errors in the ensemble configuration. In practice, significant variance reduction can be achieved with any reasonable trial functions.

For evaluating the ground-state expectation value of operators other than the Hamiltonian, a simple perturbative estimate is most convenient,[5]

$$\langle\mathcal{O}\rangle\equiv\frac{\langle\Psi_0|\mathcal{O}|\Psi_0\rangle}{\langle\Psi_0|\Psi_0\rangle}\simeq 2\frac{\langle\Phi|\mathcal{O}|\Psi_0\rangle}{\langle\Phi|\Phi\rangle}+O((\Psi_0-\Phi)^2)$$
$$\simeq 2\frac{1}{n}\sum_{i=1}^{n}\mathcal{O}(x^i)-\frac{1}{k}\sum_{i=1}^{k}\mathcal{O}(x_0^i)\ . \tag{3.10}$$

In this case, the variance cannot be made zero even if Φ were exact and, in general, the variance associated with the expectation value of an arbitrary operator is greater than that of the Hamiltonian.

Finally, since $\nabla_jE_j^a$ commutes with the individual kinetic and potential energy terms of H, one can readily show that, by applying Ω to (3.2), which defines the guided-random-walk algorithm, the resulting wave function Ψ is gauge invariant at any time step, if the trial function Φ is gauge invariant.

IV. THE TRIAL FUNCTION

To devise a reasonable trial function for guiding the random walks, it is useful to examine two limiting cases

where the ground state is known exactly.

In the strong-coupling limit of $g \to \infty$, corresponding to $\lambda \to 0$, the ground-state wave function and energy of the lattice Hamiltonian can be obtained perturbatively in powers of λ:

$$\Psi_0 = 1 + \tfrac{2}{3}\lambda \sum_p \cos(\tfrac{1}{2}B_p) + O(\lambda^2) \tag{4.1}$$

$$\approx \prod_p \exp[\tfrac{2}{3}\lambda \cos(\tfrac{1}{2}B_p)] + O(\lambda^2) , \tag{4.2}$$

$$\varepsilon_0 \equiv E_0/N = \lambda - \tfrac{1}{6}\lambda^2 + O(\lambda^4) , \tag{4.3}$$

where $N = 3L^3$ is the number of plaquettes (or links) in an L^3-site lattice. Thus, the strong-coupling lattice ground state is dominated by independent plaquette excitations[2] and has the form of a product of single-plaquette functions.

In the weak-coupling limit of $g \to 0$, and hence $\lambda \to \infty$, the lattice Hamiltonian can be rewritten in terms of the scaled variables $\tilde{A}_l^a = \sqrt{\lambda} A_l^a$, and expanded in a power series in λ^{-1}. This procedure yields a leading kinetic energy term which is the ordinary flat-space Laplacian and a leading potential term which is quadratic in the scaled plaquette variable $\tilde{B}_p = \sqrt{\lambda} \mid B_p^a \mid$, where, to leading order in λ^{-1}, B_p^a is just the lattice of A_l^a. In the limit, the Hamiltonian reduces to that of a triplet of free U(1) gauge fields on the lattice. The ground-state energy per plaquette is given by

$$\varepsilon_0 = \tfrac{3}{2} C_0 \sqrt{\lambda} + O(\lambda^0) , \tag{4.4}$$

and the corresponding ground-state wave function is a multivariate Gaussian function of the B_p^a's with relatively weak off-diagonal terms:[4]

$$\Psi_0 = \exp\left[-\sqrt{\lambda} \sum_{\mathbf{n},\mathbf{n}'} \sum_{j,a} \tfrac{1}{2} B_j^a(\mathbf{n}) \Gamma(\mathbf{n}-\mathbf{n}') \tfrac{1}{2} B_j^a(\mathbf{n}') \right] , \tag{4.5}$$

where j sums over the three plaquettes at each site $\mathbf{n}$ and where the constants C_0 and $\Gamma(0)$, depending on the size of the lattice, have values 0.7479, 0.7934, 0.7958, 0.7959, and 0.3562, 0.4281, 0.4509, and 0.4552, respectively for $L = 2$, 4, 10, and 50. Thus, if one were to approximate Ψ_0 in this limit by retaining only the dominant diagonal terms, one would again obtain a product of single-plaquette functions.

These considerations suggest that a reasonable trial function for guiding the random walks for all values of λ is a gauge-invariant, product function of the form

$$\Phi = \prod_p f(B_p) , \tag{4.6}$$

where $f(B)$ can be determined variationally by minimizing the energy functional

$$\varepsilon[f] = \frac{1}{N} \frac{\langle \Phi \mid H\Phi \rangle}{\langle \Phi \mid \Phi \rangle} . \tag{4.7}$$

For a given Hamiltonian and a "Jastrow-type" trial function of the form (4.6), the determination of the optimal single-plaquette functin f is a standard problem in variational many-body theory.[19,20] For example, in the case of a two-dimensional lattice, one can readily show that the optimal choice for f is the ground state of the single-plaquette Hamiltonian

$$\psi_0 = se_2(B/4, -4\lambda)/\sin(B/2),$$

where se_2 is a Mathieu function (see the Appendix). In the physical case of a three-dimensional lattice, although the optimal choice for f is not known, a cluster expansion of (4.7) suggests that, in the strong-coupling limit, the optimal f must be $\simeq \psi_0$. (Perhaps the application of hypernetted chain methods[19,20] in the present context will shed light on this problem.) In this work we find it expedient to parametrize $f(B)$ in the form

$$f(B) = \exp\left[\sum_{j=1/2,1,\ldots} \alpha_j \chi_j[\cos(\tfrac{1}{2}B)] \right] , \tag{4.8}$$

where $\chi_j[\cos(\frac{1}{2}B)]$ are the complete set of class functions of SU(2):

$$\chi_j[\cos(\tfrac{1}{2}B)] = \sin\left[\frac{2j+1}{2} B \right] \Big/ \sin(\tfrac{1}{2}B) , \tag{4.9}$$

and simply determine the coefficients α_j variationally by an exact Monte Carlo evaluation of (4.7).

The variational calculation is performed by averaging $\Phi^{-1}H\Phi$ over an ensemble of lattice configurations generated according to $\Phi^2/\langle \Phi \mid \Phi \rangle$ by the Metropolis[16] method. The explicit form for $\Phi^{-1}H\Phi$ used is

$$\Phi^{-1}H\Phi = -\tfrac{1}{2} \sum_l \left[\sum_p \left[\sum_j \alpha_j \chi_j'[\cos(\tfrac{1}{2}B_p)] \right] iE_l^a \cos(\tfrac{1}{2}B_p) \right]^2 + 2 \sum_p \left[\sum_j j(j+1)\alpha_j \chi_j[\cos(\tfrac{1}{2}B_p)] \right] + \lambda \sum_p [1 - \cos(\tfrac{1}{2}B_p)] , \tag{4.10}$$

where χ_j' denotes derivative with respect to its argument. The evaluation of the electric or kinetic energy, particularly the first term on the right-hand side of (4.10), is less formidable than it appears, and is discussed in detail in the Appendix. It is worth recalling[5] that, to the extent that Φ is a good approximation to the exact ground state, $\Phi^{-1}H\Phi$ will be close to being a zero-variance estimator of the ground-state energy. Thus although it is possible to eliminate the complicated first term on the RHS of (4.10) by use of the Jackson-Feenberg form of the kinetic energy (see the Appendix), this will in general result in greater variance for evaluating the ground-state energy and is therefore undesirable from the point of view of doing Monte Carlo calculations.

Since the ground state has the form (4.2) in the strong-coupling limit, we begin the variational calculation by keeping only the first, $\chi_{1/2}$, term in the expansion (4.8). The adequacy of this trial function was then checked by

including the next, χ_1, term in the minimization process. It is found that, even in the fairly weak-coupling region of $\lambda \simeq 3$, the resulting improvement in energy is slight. Since there is a tradeoff between the quality of the trial function and the ease with which it can be generated for guiding the random walks, we conclude that, in the present case, a simple one-parameter trial function of the form

$$f(B_p)=\exp[\alpha \cos(\tfrac{1}{2}B_p)] , \tag{4.11}$$

which has been considered previously by many authors,[21–24] is also adequate for our purpose. More importantly, as a byproduct of our exact calculation we are able to assess the extent to which a trial function of the product form (4.6), with f given by (4.11), is a good approximation to the true ground state.

From our discussions of the strong- and weak-coupling limits, we can expect

$$\alpha=\tfrac{2}{3}\lambda, \quad \text{for } \lambda \ll 1 \tag{4.12}$$

and

$$\alpha \simeq 2\Gamma(0)\sqrt{\lambda} , \quad \text{for } \lambda \gg 1 . \tag{4.13}$$

V. RESULTS

In the actual calculation, we represent each element of SU(2) by a quarternion $x^\mu=(x^0,x^a)$,

$$U=\cos(\tfrac{1}{2}\rho)-i\tau^a\hat{n}^a\sin(\tfrac{1}{2}\rho)=x^0-i\tau^a x^a , \tag{5.1}$$

where $x^0x^0+x^ax^a=1$, and identify the product of two SU(2) matrices as quarternion multiplication:

$$U(x)U(y)=(x^0y^0-x^ay^a)-i\tau^a(x^0y^a+y^0x^a+\epsilon^{abc}x^by^c) . \tag{5.2}$$

In this representation the trace of U_p is just $2x_p^0$, and it is unnecessary to compute the "spatial" part x_p^a. To generate a Gaussian-distributed quarternion around the identity element with zero mean and variance $\sigma^2 \to 0$, we simply generated three normal random variants A^1,A^2,A^3, with zero mean, variance σ^2, and set

$$x^\mu=(\cos(\tfrac{1}{2}\rho),(A^a/\rho)\sin(\tfrac{1}{2}\rho)) , \tag{5.3}$$

where $\rho^2=A^aA^a$. It is likely that a direct and more efficient means of sampling such a quarternion is possible. We did not explore this question in detail.

The trial function parameter α is fixed by minimizing the variational energy (4.7) computed stochastically by averaging $\Phi^{-1}H\Phi$ over a sequence of lattice configurations generated according to Φ^2 by the Metropolis[16] method. The number of lattice configurations sampled ranges from $\sim 10^3$ for $\lambda \lesssim 1$ to $\sim 10^4$ for $\lambda \gtrsim 2$. In all cases the statistical error is computed from block averages of 100 configurations. Typically, as a function of λ, the energy is calculated for six values of α and a parabola is fitted to obtain the minimum energy and the optimal α. For the case of a 4^3 lattice, the optimal α thus obtained as a function λ is shown in Fig. 1 and is in good agreement with the expected strong- and weak-coupling behavior (4.12) and (4.13). The resulting variational energy per plaquette is plotted as triangles in Fig. 3. On the scale of these figures, the statistical errors are much too small to be shown and the size of the plotting symbols is exaggerated for visibility. The numerical values of α, the variational ground-state energy, and the plaquette expectation value $\langle \cos(\frac{1}{2}B_p)\rangle$, are presented in Tables I and II.

Since the lattice used is only 4^3, it is of interest to assess the effect of finite lattice sizes. For this purpose we performed variational calculations using the discrete icosahedral subgroup of SU(2) for lattice sizes up to 16^3. The resulting variational energies at $\lambda=0.6$, 1.0, 1.6, and 2.5 for a 16^3 lattice are plotted as crosses on Fig. 3. The numerical values for the ground-state energy and the plaquette expectation value for three lattice sizes 4^3, 8^3, and 16^3, are presented in Table III. The effect of finite lattice size on the variational calculation is thus demonstrably small.

With Φ thus defined by $\alpha(\lambda)$, the exact Monte Carlo calculation with trial function guidance proceeds as outlined in Sec. III: For a chosen value of Δt, an ensemble of N_p lattice configurations is first generated according to Φ^2 and successive generations of ensembles are then evolved by replications and guided random walks. To determine the normalization energy E_N, the constant E in the replication factor $w(\mathbf{x})$ is adjusted after each time step to stabilize the average configuration population in each generation at the initial value of N_p. (For a discussion of the potential bias that can result from too frequent an adjustment of E, see Ref. 4.) From our previous experience with U(1) calculations, we use $N_p=10$, although a smaller value may also be adequate. In a typical run of 2000 to 8000 time steps (depending on the value of λ), after discarding the first few hundred generations which have not equilibrated to the stationary distribution, observables are again averaged over blocks of 50 time steps (≈ 500 configurations to assure statistical independence. The computation is then repeated for successively smaller values of Δt using the equilibrated configurations from the previous Δt calculation as a starting point. The resulting time step

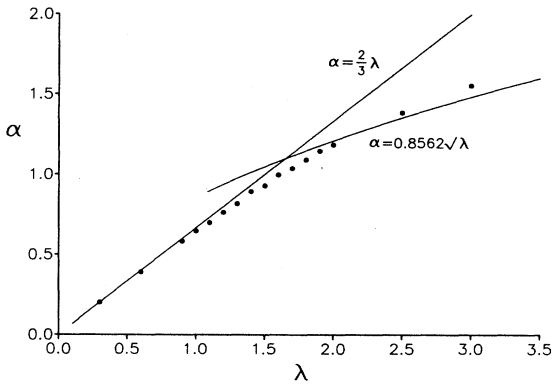

FIG. 1. The optimal trial function parameter α as determined by a Monte Carlo variational calculation as a function of the coupling constant λ for a 4^3 lattice. The solid curves are the expected strong- and weak-coupling behaviors. The statistical error in α is smaller than the size of the plotting symbols (see Table I).

TABLE I. Numerical values for the trial function parameter α, the variational energy $\varepsilon_{\rm var}$, the exact ground-state energy ε_0, and the cubic spline fit to the exact energy $\varepsilon_{\rm fit}$ at 16 selected values of λ. Statistical errors are enclosed in parentheses.

λ	α	$\varepsilon_{\rm var}$	ε_0	$\varepsilon_{\rm fit}$
0.3	0.197(1)	0.285 10(001)	0.285 10(006)	0.285 12
0.4	0.262(1)	0.373 65(001)	0.373 56(011)	0.373 56
0.5	0.326(1)	0.459 03(002)	0.458 72(006)	0.458 70
0.6	0.393(2)	0.541 36(002)	0.540 50(009)	0.540 55
0.7	0.453(2)	0.620 73(004)	0.619 43(011)	0.619 44
0.8	0.516(4)	0.697 27(006)	0.695 27(013)	0.695 16
0.9	0.583(4)	0.770 79(005)	0.767 42(022)	0.767 34
1.0	0.646(3)	0.841 71(007)	0.835 81(028)	0.836 30
1.1	0.699(3)	0.909 89(008)	0.902 31(032)	0.902 55
1.2	0.763(4)	0.975 60(010)	0.966 82(042)	0.965 95
1.4	0.893(8)	1.099 13(020)	1.083 57(064)	1.083 02
1.6	0.996(5)	1.213 05(023)	1.188 09(058)	1.188 06
1.8	1.091(7)	1.318 75(020)	1.283 21(083)	1.283 60
2.0	1.186(7)	1.416 88(028)	1.378 65(102)	1.372 41
2.5	1.385(5)	1.636 15(033)	1.576 50(079)	1.576 28
3.0	1.554(5)	1.825 86(070)	1.764 00(112)	1.765 06

size dependence of E_N/N and E_T/N ($N=3L^3$) for three selected values of λ is displayed in Fig. 2. The solid lines are linear least-square fits to the data. The convergence of E_N/N and E_T/N as $\Delta t\to 0$ is particularly evident. The systematic trend from $\lambda=0.8$ to $\lambda=3.0$ also clearly demonstrates the fact that in the region where Φ is a good approximation to Ψ_0, both statistical errors and errors of Δt extrapolation are simultaneously reduced. In the final analysis, we combine the statistics of E_N and E_T by fitting both sets of data with two straight lines having a common intercept at $\Delta t=0$. The ground-state energies thus obtained are reported in Table I. Such a high level of precision is difficult to attain in a conventional Monte Carlo calculation without a trial function.

TABLE II. Numerical values for the plaquette expectation value $\langle\cos(\frac{1}{2}B_p)\rangle$ at 16 selected values of λ evaluated by using the variational trial function, $\langle\cos\rangle_{\rm var}$, the perturbative estimate (3.10), $\langle\cos\rangle_{\rm pert}$, and by differentiating the fitted ground-state energy, $\langle\cos\rangle_{\rm diff}$. Statistical errors are enclosed in parentheses.

λ	$\langle\cos\rangle_{\rm var}$	$\langle\cos\rangle_{\rm pert}$	$\langle\cos\rangle_{\rm diff}$
0.3	0.098 2(04)	0.096 6(44)	0.0994
0.4	0.129 6(04)	0.130 6(46)	0.1319
0.5	0.159 7(04)	0.165 1(25)	0.1655
0.6	0.192 4(04)	0.192 6(29)	0.1965
0.7	0.220 2(04)	0.229 0(23)	0.2262
0.8	0.248 5(05)	0.251 3(26)	0.2605
0.9	0.278 6(06)	0.293 4(31)	0.2952
1.0	0.305 8(06)	0.326 0(33)	0.3243
1.1	0.331 6(06)	0.348 2(29)	0.3511
1.2	0.357 0(07)	0.374 0(35)	0.3819
1.4	0.407 4(07)	0.440 8(35)	0.4464
1.6	0.452 8(08)	0.485 4(30)	0.5009
1.8	0.490 5(08)	0.549 1(36)	0.5413
2.0	0.525 8(11)	0.565 5(35)	0.5687
2.5	0.591 5(05)	0.636 6(20)	0.6119
3.0	0.638 5(05)	0.665 6(25)	0.6277

In Fig. 3, the exact ground-state energy is plotted as solid circles. In the strong-coupling regime of $\lambda\ll 1.0$, the variational and exact energies are in excellent agreement with each other and with the strong-coupling expansion. In the weak-coupling regime of $\lambda\gg 1.0$, the exact energy is significantly lower than the variational results. Moreover, in this region, the exact energy is well described by the weak-coupling expansion

$$\varepsilon_0=\tfrac{3}{2}C_0\sqrt{\lambda}-C_1-C_2/\sqrt{\lambda}\ , \tag{5.4}$$

where C_0 is as defined in the last section and where C_1 and C_2, though in principle calculable, are more easily determined from the data: $C_1\approx 0.24$ and $C_2\approx 0.09$. This, together with the result for the plaquette expectation value, to be described shortly, convincingly demonstrate that the proposed stochastic algorithm is capable of converging to the proper ground state by generating plaquette correlations that were initially absent in the trial function.

As a more sensitive probe of the ground-state wave

TABLE III. The variational ground-state energy and plaquette expectation value calculated with the discrete icosahedral subgroup of SU(2) as a function of lattice size at four selected values of λ. Statistical errors are enclosed in parentheses.

λ	L^3	$\varepsilon_{\rm var}$	$\langle\cos\rangle_{\rm var}$
0.6	4^3	0.541 30(010)	0.192 50(109)
	8^3	0.541 35(005)	0.192 68(053)
	16^3	0.541 36(002)	0.192 47(020)
1.0	4^3	0.841 69(028)	0.305 43(105)
	8^3	0.841 79(010)	0.305 38(038)
	16^3	0.841 66(007)	0.305 69(026)
1.6	4^3	1.212 03(102)	0.451 44(155)
	8^3	1.213 90(036)	0.451 52(056)
	16^3	1.213 74(018)	0.451 01(031)
2.5	4^3	1.635 79(241)	0.591 64(178)
	8^3	1.636 97(063)	0.590 91(051)
	16^3	1.636 24(033)	0.590 64(024)

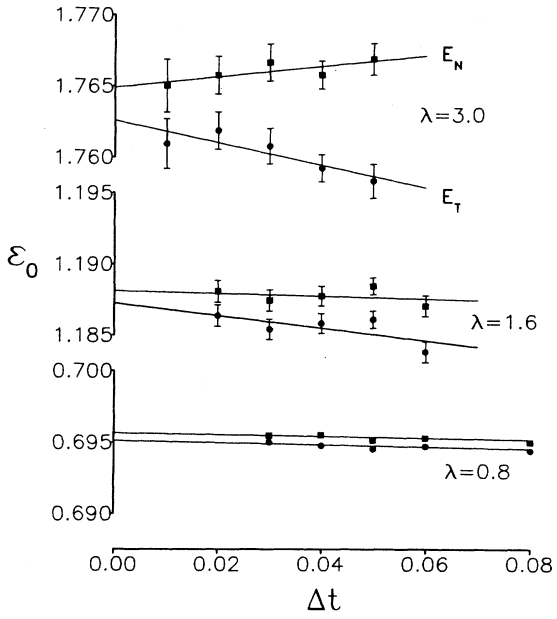

FIG. 2. The calculated ground-state energy per plaquette for a 4^3 lattice at selected values of λ as a function of time step size Δt. The normalization and the trial energies are indicated by the solid squares and the solid circles, respectively. The straight lines are linear least-squares fits to the data.

function, it is useful to consider the plaquette operator $\cos(\frac{1}{2}B_p)$. Its expectation can either be obtained via the perturbative estimate, (3.10), or by relating it to the derivative of the ground-state energy:

$$\langle\cos(\tfrac{1}{2}B_p)\rangle \equiv \frac{1}{N}\frac{1}{\langle\Psi_0|\Psi_0\rangle}\left\langle\Psi_0\left|\sum_p\cos(\tfrac{1}{2}B_p)\right|\Psi_0\right\rangle$$
$$=\frac{1}{\langle\Psi_0|\Psi_0\rangle}\left\langle\Psi_0\left|\left[1-\frac{1}{N}\frac{\partial H}{\partial\lambda}\right]\right|\Psi_0\right\rangle$$
$$=1-\frac{d\varepsilon_0}{d\lambda}\,. \tag{5.5}$$

The expectation values $\langle\cos(\frac{1}{2}B_p)\rangle$ calculated according to (3.10) as a function of λ are given numerically in Table II and are plotted as solid circles on Fig. 4. In this case, since the variance no longer diminishes in proportion to $(\Psi_0-\Phi)$, as in the case of the Hamiltonian, both statistical errors and errors of extrapolation are substantial, even in the strong-coupling limit. In comparison, the variance associated with the Hamiltonian in this limit is smaller by at least an order of magnitude. To calculate the derivative of ε_0, we first smooth out the ground-state energy by performing a weighted least-square fit to the data with cubic splines. The resulting fitted values are displayed in Table I. With the exception of the data point at $\lambda=2.0$ (for which we have no explanation) the fit is generally within one standard derivation of the exact ground-state energy. The plaquette expectation value obtained by differentiating the cubic splines are given in Table II and are plotted as a dashed curve in Fig. 4. The values of $\langle\cos(\frac{1}{2}B_p)\rangle$ determined by these two independent methods are generally in good agreement with each other. In both the strong- and the weak-coupling limit the data are well described by just the leading term in the corresponding expansion. In particular, it should be noted that $\langle\cos(\frac{1}{2}B_p)\rangle$ persists in its weak-coupling behavior all the way down to $\lambda\approx1.7$ and then rather sharply changes over to its strong-coupling form. Such a crossover behavior, in retrospect, is also evident in the ground-state energy. This suggests that it is the ground state itself that is rapidly changing over to the strong-coupling limit at a rather modest coupling of $g^2/4\pi=(2\pi\sqrt{\lambda})^{-1}\approx0.12$. Since we have yet to calculate physical observables, we are not in a position to identify this as the onset of confinement. Nevertheless, it should be noted that the occurrence of a crossover at this particular coupling is consistent with a similar phenomenon seen in Lagrangian calculations.[1]

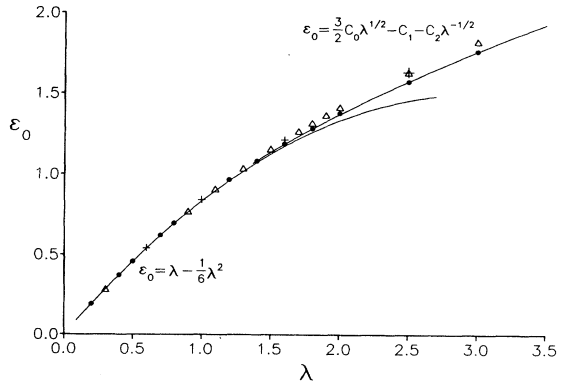

FIG. 3. The ground-state energy per plaquette as a function of the coupling constant λ. The triangles and the solid circles denote, respectively, the variational and the exact Monte Carlo results for a 4^3 lattice. The crosses are variational results calculated using the discrete icosahedral subgroup of SU(2) for a 16^3 lattice. The expected strong- and weak-coupling behaviors are as indicated. The constant C_0 in the weak-coupling limit was derived but the constants C_1 and C_2 were simply obtained by fitting the exact energies at $\lambda\geq1.4$.

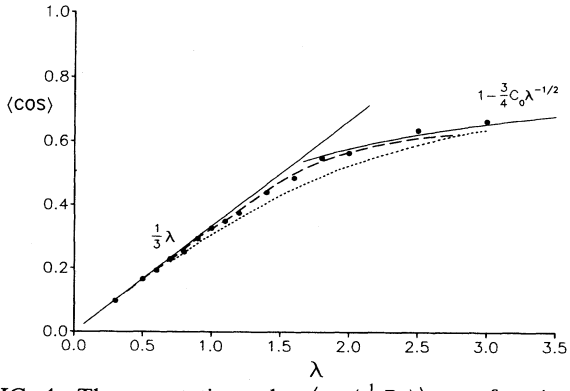

FIG. 4. The expectation value $\langle\cos(\frac{1}{2}B_p)\rangle$ as a function of the coupling constant λ. The solid dots denote Monte Carlo results using the perturbative estimate (3.10). The dashed curve is obtained by differentiating the ground-state energy as explained in the text. The dotted curve is an interpolation of the variational results.

For comparison, the variational results for $\langle \cos(\frac{1}{2}B_p) \rangle$ are plotted (after interpolation) as a dotted curve in Fig. 4. Its only deficiency is that it smoothed out the sharp crossover.

This entire calculation required approximately 80 hours on the FPS-164 array processor at the Oak Ridge National Laboratory.

VI. CONCLUSIONS AND FUTURE PROSPECTS

In this work we have explicitly shown that the SU(2) Hamiltonian lattice gauge theory is equivalent to a nonrelativistic quantum many-body problem and have devised a specific Monte Carlo algorithm for sampling its ground state. To the extent that the guiding trial function formed by a product of single-plaquette functions is a reasonable approximation to the exact ground state, the guided-random-walk algorithm was shown to be an efficient means of calculating the ground-state energy. Our results for the plaquette expectation value also suggest that the ground state changes sharply from its weak-coupling behavior to that of the strong coupling at $\lambda \approx 1.7$, which is consistent with a similar phenomenon observed in Lagrangian calculations.

The identification of a Hamiltonian lattice gauge theory as a many-body problem holds for any SU(N) gauge group[4] and provides a new perspective for the study of lattice gauge theories. For example, the well-known Bijl-Feynman[20] variational method for studying low-lying collective excitations of a many-particle system can now be applied to the study of the glueball spectrum. This approach has the advantage of dealing with the Hamiltonian operator directly rather than e^{-tH}, which is used in the Lagrangian variational calculation. We are currently investigating the mass gap in SU(2) from this perspective.

This identification also invites us to explore other many-body techniques for the study of lattice gauge theory. As we have outlined in the Appendix, much of the existing variational many-body machinery probably has analogs in variational lattice gauge theory. Although we have shown that the variational calculation with trial function (4.11) tends to smooth out the sharp crossover, it remains possible that a more refined variational study can remedy this deficiency. In any case, a systematic development of a "hypernetted surfaces" approach to lattice gauge theory would be very interesting and would measurably expand the scope of many-body theory.

The present Hamiltonian approach is equally suited to the study of other physical observables such as the quark-quark potential. The potential is presumably directly calculable by placing two sources at different lattice sites. In the present formalism, there is no temperature effect due to a finite temporal lattice size and no need to evaluate large Wilson loops.

We have found the use of discrete subgroups very valuable in doing variational calculations. The use of a group table in place of quarternion multiplication enables us to check finite-size effects in lattices as large as 16^3 on a VAX 11/780 computer. It would be extremely interesting to develop a discrete Monte Carlo algorithm for sampling the exact ground state. In the guided-random-walk algorithm, the drift step generated by the trial function inevitably falls "between the cracks" of the icosahedral subgroup; one must therefore decide which of the nearby group elements to use. We have yet to devise a satisfactory resolution to this problem.

Finally, the guided-random-walk algorithm, as outlined in this work, is directly applicable to the case of SU(3) with only straightforward numerical complications.

Note added in proof. After submission of this paper we learned of the recent work of Heys and Stump[28] on Green's-function Monte Carlo calculations on the SU(2) and U(1) lattice gauge theories. Conclusions reached in that paper are very similar to those found in ours.

ACKNOWLEDGMENTS

We thank the Nuclear Theory Group at the Oak Ridge National Laboratory for the use of their FPS-164 array processor. This work was supported in part by the National Science Foundation Grants Nos. PHY 83-40400, PHY 82-15500, PHY 82-07332, and PHY 82-08439, and the Department of Energy Contract No. DE-AC02-76 ER 03074.

APPENDIX

In this appendix, we discuss three topics of related interest: the single-plaquette Hamiltonian, a variational cluster expansion, and the evaluation of the kinetic energy. The single-plaquette Hamiltonian is exactly solvable in terms of Mathieu functions. Its solution illustrates many technical manipulations which are important for the study of the full lattice. The cluster expansion provides a systematic basis for studying lattice gauge theories variationally. In this brief appendix we seek to demonstrate that many of the standard techniques of nonrelativistic many-body theory[19,20] might be fruitfully applied in this new context. Finally, the evaluation of the kinetic energy in its original form is essential for variance reduction and the technical discussion is aimed at those who wish to pursue this calculation further.

1. Single-plaquette Hamiltonian

The single-plaquette Hamiltonian is given by

$$h=\sum_{l=1}^{4} \tfrac{1}{2} E_l^a E_l^a + \lambda[1-\cos(\tfrac{1}{2}B_p)] , \tag{A1}$$

where $\cos(\frac{1}{2}B_p)=\frac{1}{2}\,\mathrm{tr}U_p$,

$$U_p = U_1 U_2 U_3{}^{-1} U_4{}^{-1} = \cos(\tfrac{1}{2}B_p) - i\hat{n}_p^a \tau^a \sin(\tfrac{1}{2}B_p) , \tag{A2}$$

and where

$$E_l^a U_{l'} = \tfrac{1}{2}\tau^a U_l \delta_{l,l'} , \tag{A3}$$

$$E_l^a U_{l'}{}^{-1} = -U_l{}^{-1} \tfrac{1}{2}\tau^a \delta_{l,l'} . \tag{A4}$$

To solve the eigenvalue problem

$$h\psi = \varepsilon\psi , \tag{A5}$$

let $\psi=\psi(B_p)$. Since E_l^a are first-order differential operators,

$$E_1^a\cos(\tfrac{1}{2}B_p)=\tfrac{1}{2}\,\mathrm{tr}(\tfrac{1}{2}\tau^a U_p)\ ,$$
$$-\sin(\tfrac{1}{2}B_p)\tfrac{1}{2}E_1^aB_p=-i\tfrac{1}{2}\hat{n}_p^a\sin(\tfrac{1}{2}B_p)\ ,$$

and therefore

$$E_1^aB_p=i\hat{n}_p^a\ . \tag{A6}$$

Similarly for E_4^a,

$$E_4^aB_p=-i\hat{n}_p^a\ . \tag{A7}$$

In the case of E_2^a,

$$\begin{aligned}E_2^a\cos(\tfrac{1}{2}B_p)&=\tfrac{1}{2}\,\mathrm{tr}(U_1\tfrac{1}{2}\tau^aU_2U_3{}^{-1}U_4{}^{-1})\\&=\tfrac{1}{2}\,\mathrm{tr}(\tfrac{1}{2}\tau^aU_1{}^{-1}U_pU_1)\ ,\\\Rightarrow E_2^aB_p&=i[R^{ab}(U_1)\hat{n}_p^b]\ ,\end{aligned} \tag{A8}$$

where $R^{ab}(U_1)\hat{n}_p^b$ is the unit vector $\hat{n}_p^a$ rotated by an amount ρ_1 in the direction (θ_1,ϕ_1). Likewise for E_3^a,

$$E_3^aB_p=-i[R^{ab}(U_4)\hat{n}_p^b]\ . \tag{A9}$$

Furthermore, with no sum over l,

$$\begin{aligned}&E_l^aE_l^a\cos(\tfrac{1}{2}B_p)=\tfrac{1}{2}\,\mathrm{tr}(\tfrac{1}{2}\tau^a\tfrac{1}{2}\tau^aU_p)\ ,\\&-\tfrac{1}{4}\cos(\tfrac{1}{2}B_p)(E_l^aB_p)(E_l^aB_p)-\tfrac{1}{2}\sin(\tfrac{1}{2}B_p)E_l^aE_l^aB_p\\&\qquad=\tfrac{3}{4}\cos(\tfrac{1}{2}B_p)\\&\qquad\Rightarrow E_l^aE_l^aB_p=-\cot(\tfrac{1}{2}B_p)\ .\end{aligned} \tag{A10}$$

Hence, it follows that, for each l,

$$\begin{aligned}E_l^aE_l^a\psi(B_p)&=\psi''(B_p)(E_l^aB_p)(E_l^aB_p)+\psi'(B_p)E_l^aE_l^aB_p\ ,\\&=-\psi''(B_p)-\cot(\tfrac{1}{2}B_p)\psi'(B_p)\ ,\\&=-\frac{1}{\sin^2(\frac{1}{2}B_p)}\left[\frac{\partial}{\partial B_p}\sin^2(\tfrac{1}{2}B_p)\frac{\partial}{\partial B_p}\right]\psi(B_p)\ ,\end{aligned} \tag{A11}$$

and (A5) reduces to

$$\begin{aligned}-2\frac{1}{\sin^2(\frac{1}{2}B_p)}&\left[\frac{\partial}{\partial B_p}\sin^2(\tfrac{1}{2}B_p)\frac{\partial}{\partial B_p}\right]\psi(B_p)\\&+\lambda[1-\cos(\tfrac{1}{2}B_p)]\psi(B_p)=\varepsilon\psi(B_p)\ .\end{aligned} \tag{A12}$$

This radial equation can be solved in the usual manner by setting $\psi(B_p)=R(B_p)/\sin(\frac{1}{2}B_p)$, thus yielding

$$\left[-2\frac{\partial^2}{\partial B_p{}^2}+\lambda[1-\cos(\tfrac{1}{2}B_p)]\right]R=(\varepsilon+\tfrac{1}{2})R\ , \tag{A13}$$

which is a form of the Mathieu equation.[25] A more circuitous derivation of (A13) was previously given in Ref. 26.

Since $\psi_0(B_p)$ must be symmetric in its argument, periodic with period 4π, and nonsingular everywhere, $R_0(B_p)$ must be *antisymmetric* with period 4π, and vanish at $B_p=0$. This uniquely identifies the ground state of (A13) as the Mathieu function[25] $se_2(B_p/4,-4\lambda)$ with energy

$$\varepsilon_0=\lambda-\tfrac{1}{6}\lambda^2+\tfrac{5}{432}\lambda^4+\cdots\ ,\quad \lambda\ll 1 \tag{A14}$$
$$=\tfrac{3}{2}\sqrt{\lambda}-\tfrac{21}{32}+\cdots\ ,\quad \lambda\gg 1\ . \tag{A15}$$

The corresponding ground state

$$\psi_0=se_2(B_p/4\lambda)/\sin(\tfrac{1}{2}B_p)$$

has the expansion

$$\psi_0=1+\frac{\lambda}{3}[2\cos(\tfrac{1}{2}B_p)]+\frac{\lambda^2}{24}[4\cos^2(\tfrac{1}{2}B_p)-1]+\cdots\ ,\quad \lambda\ll 1 \tag{A16}$$
$$=\exp\{-\tfrac{1}{2}\sqrt{\lambda}(\tfrac{1}{2}B_p)^2\}\ ,\quad \lambda\gg 1\ . \tag{A17}$$

The single-plaquette Hamiltonian is analytically solvable in terms of Mathieu functions for the general case of a U(N) gauge group. The corresponding "radial" wave function is likewise completely antisymmetric in its arguments and may be regarded as the ground state of a N-fermion problem. The interested reader can consult Ref. 27.

2. Cluster expansion

This section generalizes the discussion in Ref. 4 for the case of U(1) to SU(2). It should be clear from the following that the extension to the case of SU(N) is straightforward.

In evaluating the energy functional (4.7), the kinetic energy can either be evaluated directly,

$$\left\langle\Phi\left|\sum_l\tfrac{1}{2}E_l^aE_l^a\right|\Phi\right\rangle=\tfrac{1}{2}\sum_l\int d\mathbf{x}[(E_l^a\ln\Phi)(E_l^a\ln\Phi)+(E_l^aE_l^a\ln\Phi)]\Phi^2(\mathbf{x})\ , \tag{A18}$$

or by commuting operators, $\langle 0\,|\,\Phi E_l^aE_l^a\Phi\,|\,0\rangle=-\langle 0\,|\,(E_l^a\Phi)(E_l^a\Phi)\,|\,0\rangle$, to give

$$\left\langle\Phi\left|\sum_l\tfrac{1}{2}E_l^aE_l^a\right|\Phi\right\rangle=\tfrac{1}{2}\sum_l\int d\mathbf{x}[-(E_l^a\ln\Phi)(E_l^a\ln\Phi)]\Phi^2(x)\ . \tag{A19}$$

The average of these two yield the Jackson-Feenberg form of the kinetic energy:

$$\left\langle\Phi\left|\sum_l\tfrac{1}{2}E_l^aE_l^a\right|\Phi\right\rangle=\tfrac{1}{4}\sum_l\int d\mathbf{x}(E_l^aE_l^a\ln\Phi)\Phi^2(\mathbf{x})\ . \tag{A20}$$

For a trial function of the product form (4.6), the use of (A20) allows us to express the energy functional concisely as

$$\varepsilon[f]=\int dU_pG(B_p)\left[-\frac{1}{\sin^2(\frac{1}{2}B_p)}\left[\frac{\partial}{\partial B_p}\sin^2(\tfrac{1}{2}B_p)\frac{\partial}{\partial B_p}\right]\ln f+\lambda[1-\cos(\tfrac{1}{2}B_p)]\right]\ , \tag{A21}$$

where $U_p = U_1 U_2 U_3{}^{-1} U_4{}^{-1}$ is a particular plaquette formed by the four links U_1 to U_4, where

$$G(B_p) = f^2(B_p) \frac{1}{\langle \Phi \mid \Phi \rangle} \int dU_5 \cdots dU_N \prod_{q \neq p} f^2(B_q), \tag{A22}$$

and is normalized via

$$\int dU_1 dU_2 dU_3 dU_4 G(B_p) = \int dU_p G(B_p) = 1 , \tag{A23}$$

and where the normalized, invariant group measure is given by

$$dU = d(U'U) = d(UU') = \frac{1}{16\pi^2} 4 \sin^2(\tfrac{1}{2}\rho) d\rho \sin\theta \, d\theta \, d\phi . \tag{A23'}$$

A useful technique for evaluating $G(B_p)$ is to develop a cluster expansion[19] in power of the bond function

$$b(B_p) = f^2(B_p) - 1 . \tag{A24}$$

Such an expansion is clearly reasonable in the strong-coupling limit where f is expected to be close to one and higher powers of b are correspondingly small. Substituting (A24) in (A22) yields

$$G(B_p) = f^2(B_p) \frac{1}{\langle \Phi \mid \Phi \rangle} \int dU_5 \cdots dU_N \left[1 + \sum_{q \neq p} b(B_q) + \sum_{q \neq k \neq p} b(B_q) b(B_k) + \sum_{q \neq k \neq h \neq p} b(B_q) b(B_k) b(B_h) + \cdots \right] . \tag{A25}$$

We shall refer to an integrated link variable U_i $(5 \leq i \leq N)$ in a product of bond functions as "exposed," if it occurs only once in the product. By extension, a bond function is also exposed if it contains at least one exposed link. Due to the invariance of group integration, any exposed bond can be immediately integrated via its exposed link to yield a constant. To prevent exposure, a link must be shared by at least two bonds. One can picture this requirement as simply the joining of each bond's plaquette at an edge. A product of bonds can therefore escape exposure only if its plaquettes form one or more closed surfaces. Hence, in the expansion (A25), all contributions to $G(B_p)$ which are not simply proportional to $f^2(B_p)$ are those corresponding to connected, closed surfaces surrounding the plaquette U_p.

In the case of a two-dimensional lattice, if no boundary conditions are prescribed, then there are no closed surfaces. In this case, exposure is unavoidable and the entire expansion in (A25) simply collapses against the denominator $\langle \Phi \mid \Phi \rangle$ to yield

$$G(B_p) = \frac{1}{\langle f \mid f \rangle} f^2(B_p) \tag{A26}$$

exactly. Substituting this back into (A21) gives

$$\varepsilon[f] = \frac{\langle f \mid h \mid f \rangle}{\langle f \mid f \rangle} , \tag{A27}$$

where h is the single-plaquette Hamiltonian given by (A12). Hence, in *two dimensions,* the product trial function of the form (4.6) is optimized by taking f to be the ground state of the single-plaquette Hamiltonian.

In three dimensions, the first nontrivial term in the expansion (A25) is a product of five bonds, whose plaquettes, together with U_p, for a closed cubic surface with unit volume. The next contribution is a product of nine bonds forming a rectangular surface with 2 units of volume, and so on. Since the cluster expansion for $G(B_p)$ begins at such a high order, in the strong-coupling limit, it is a reasonable approximation to retain only the zero-order contribution. In this case $G(B_p)$ is proportional to $f^2(B_p)$ and the normalization requirement (A23) would again lead us to (A26) and (A27). Hence, one can expect that in the strong-coupling limit, the optimal choice for f must also be the ground state of the single-plaquette Hamiltonian.

To characterize the optimal product trial function in three dimensions more completely, one must develop techniques for enumerating, classifying, and summing all possible closed surface contributions in a lattice. This very interesting problem is beyond the scope of the present paper.

3. Evaluating the kinetic energy

In Monte Carlo calculations, as argued in Sec. IV, it is important to evaluate the kinetic energy directly as given by (A18). This entails the evaluation of the nonlocal first term on the right-hand side of (A18). For a trial function of the general form (4.8), this is given by

$$\tfrac{1}{2} \sum_l (E_l^a \ln\Phi)(E_l^a \ln\Phi) = -\tfrac{1}{2} \sum_l \left[\sum_l \left[\sum_j \alpha_j \chi_j'[\cos(\tfrac{1}{2} B_p)] \right] i E_l^a \cos(\tfrac{1}{2} B_p) \right]^2 . \tag{A28}$$

By representing each SU(2) element as a quarternion, $U = x^0 - i\tau^a x^a$, as advocated in Sec. V, the effect of iE_l^a on $\cos(\frac{1}{2} B_p)$ is just

$$iE_l^a \cos(\tfrac{1}{2} B_p) = \tfrac{1}{2} x_{p,l}^a \quad \text{if } l \in p ,$$
$$= 0 \quad \text{otherwise} ;$$

where, depending on the relative position of l in the plaquette p, as shown in part 1 of this appendix,

$$x^a_{p,1} = -x^a_{p,4} = x^a_p ,$$
$$x^a_{p,2} = R^{ab}(U_1) x^b_p ,$$
$$x^a_{p,3} = -R^{ab}(U_4) x^b_p ,$$

where

$$R^{ab}(U) y^b = (x^0 x^0 - x^c x^c) y^a + 2(x^0 \varepsilon^{abc} y^b x^c + x^c y^c x^a) .$$

Hence,

$$\tfrac{1}{2} \sum_l (E^a_l \ln\Phi)(E^a_l \ln\Phi) = -\tfrac{1}{8} \sum_l \left[\sum_{p \in l} \left[\sum_j \alpha_j \chi'_j \right] x^a_{p,l} \right]^2 . \tag{A29}$$

This can be evaluated by preparing a "link accumulator" array with dimension equal to three times the number of links in the lattice. As one sweeps through the lattice evaluating plaquette variables, each x^a_p can be appropriately rotated, multiplied, and stored additively into the four slots in the accumulator associated with each plaquette's four links. At the end of the sweep, the sum of the squares of each array element in the accumulator then directly gives the right-hand side of (A29).

---

*Present address: Department of Physics, Texas A&M University, College Station, TX 77843.

†Present address: A. W. Wright Nuclear Structure Laboratory, Yale University, New Haven, CT 06511.

[1] *Lattice Gauge Theories and Monte Carlo Simulation,* edited by C. Rebbi (World Scientific, Singapore, 1983).

[2] J. Kogut and L. Susskind, Phys. Rev. D **11**, 395 (1975).

[3] M. Creutz, Phys. Rev. D **15**, 1128 (1977).

[4] S. A. Chin, J. W. Negele, and S. E. Koonin, Ann. Phys. (N.Y.) **157**, 140 (1984).

[5] D. M. Ceperly and M. H. Kalos, in *Monte Carlo Methods in Statistical Mechanics,* edited by K. Binder (Springer, New York, 1979).

[6] *Monte Carlo Methods in Quantum Problems,* edited by M. H. Kalos (Reidel, Holland, 1984).

[7] J. B. Anderson, J. Chem. Phys. **63**, 1499 (1975); **65**, 4121 (1976); **73**, 3897 (1980); **74**, 6307 (1981).

[8] P. A. Whitlock, M. H. Kalos, G. V. Chester, and D. M. Ceperley, Phys. Rev. B **19**, 5598 (1979).

[9] J. W. Moskowitz, K. E. Schmidt, M. E. Lee, and M. H. Kalos, J. Chem. Phys. **77**, 349 (1982).

[10] P. J. Reynolds, D. M. Ceperley, B. J. Alder, and W. A. Lester, J. Chem. Phys. **77**, 5593 (1982).

[11] S. E. Koonin, in *Nuclear Theory 1981,* edited by G. F. Bertsch (World Scientific, Singapore, 1983).

[12] J. W. Negele, in *Proceedings of the International Symposium on Time-Dependent Hartree-Fock and Beyond, Lecture Notes in Physics,* edited by K. Goeke and P. G. Reinhard (Springer, New York, 1979).

[13] D. W. Heys and D. R. Stump, Phys. Rev. D **28**, 2067 (1983).

[14] J. M. Normand, *A Lie Group: Rotations in Quantum Mechanics* (North-Holland, Amsterdam, 1980).

[15] R. Graham, Z. Phys. B **26**, 281 (1977).

[16] N. Metropolis, A. W. Rosenbluth, M. N. Rosenbluth, A. H. Teller, and E. Teller, Phys. Rev. **21**, 1087 (1953).

[17] M. S. Marinov and M. V. Terent'ev, Yad. Fiz. **28**, 1418 (1978) [Sov. J. Nucl Phys. **28**, 729 (1978)]; Fortschr. Phys. **27**, 511 (1979).

[18] P. Menotti and E. Onofri, Nucl. Phys. **B190**, 288 (1981).

[19] J. G. Zabolitzky, in *Advance in Nuclear Physics,* edited by J. W. Negele and E. Vogt (Plenum, New York, 1981), Vol. 12.

[20] C. E. Campbell, in *Progress in Liquid Physics,* edited by C. A. Croxton (Wiley, London, 1977).

[21] T. Hofsäss and R. Horsley, Phys. Lett. **123B**, 65 (1983).

[22] D. Horn and M. Karliner, Nucl. Phys. **B235**, 135 (1984).

[23] D. W. Heys and D. R. Stump, Phys. Rev. D **29**, 1791 (1984).

[24] E. Dagotto and A. Moreo, Phys. Rev. D **29**, 2350 (1984).

[25] *Handbook of Mathematical Functions,* edited by M. Abramowitz and I. A. Stegun, National Bureau of Standards, Applied Mathematics Series, No. 55 (U.S. G.P.O. Washington, D. C., 1964).

[26] D. Robson and D. M. Webber, Z. Phys. C **7**, 53 (1980).

[27] S. Wadia, Phys. Lett. **93B**, 403 (1980).

[28] D. W. Heys and D. R. Stump, Phys. Rev. D **30**, 1315 (1984).